THE JOURNAL OF PHYSICAL CHEMISTRY Letters

Letter

Cite This: J. Phys. Chem. Lett. 2018, 9, 3517−3524

pubs.acs.org/JPCL

Trap-Door-Like Irreversible Photoinduced Charge Transfer in a Donor−Acceptor Complex

Carlos R. Medrano[†,‡] and Cristián G. Sánchez*[,†,‡]

[†]Universidad Nacional de Córdoba, Facultad de Ciencias Químicas. Departamento de Química Teórica y Computacional, Ciudad Universitaria, X5000HUA Córdoba, Argentina

[‡]Instituto de Investigaciones Fisicoquímicas de Córdoba, Consejo Nacional de Investigaciones Científicas y Técnicas (INFIQC - CONICET), Ciudad Universitaria, X5000HUA Córdoba, Argentina

Supporting Information

ABSTRACT: For efficient conversion of light into useful energy sources, it is very important to study and describe the first steps of primary charge-transfer process in natural structures and artificial devices. The time scale of these processes in artificial photosynthetic and photovoltaic devices is on the order of femto- to picoseconds and involves vibronic coupling of electrons and nuclei and also nuclear alleviation to enhance charge separation. Here we present an atomistic description of the photoexcited electron dynamics in a noncovalently bonded system formed by an hydrogenated nanodiamond as donor and a perylene diimide as an acceptor. The complex shows extremely fast charge transfer, separation, and stabilization within 90 fs. This stabilization is purely electronic in nature. To the best of our knowledge, these results show for the first time that it is possible to stabilize charge without polaron formation or nuclear relaxation, reaching a steady state enhanced by a pure electronic reorganization.

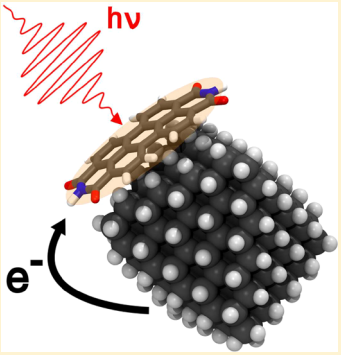

Light-induced charge transfer and subsequent charge separation are fundamental processes for a variety of phenomena including artificial and natural photosynthesis and solar energy conversion in photovoltaic cells. It is well known that the excitation of the "special pair" and the primary process in photosynthesis are followed by a series of secondary reactions involving electron transfer. These secondary reactions are faster than charge recombination processes, allowing an efficient charge separation. As a result of this process, photosynthetic organisms can obtain useful chemical redox energy from electronic excitation in the reaction center.[1]

Following nature's strategy, several dyads and triads based on porphyrin derivatives have been synthesized and studied. From the first dyads, based on porphyrin covalently linked with quinone, C_{60}, carotenoid, or aromatic imides,[2−6] to triads based on carotenoid−porphyrin−quinone or carotenoid−porphyrin−C_{60}.[7,8] The first charge separation event in these systems occurs within 3 ps to ∼40 fs.[9−13] This kind of supramolecular structures was used to fabricate single-material organic solar cells (SMOCs) for light to electricity conversion applications[14] but with low power conversion energy (PCE, record of 2.2%[15]), probably due to the fast charge recombination they present.[16]

Another approach to organic solar cells (OSCs) is bilayer heterojunctions and bulk heterojunction architectures, where the active layer is formed by a blend of donor and acceptor materials. The bulk heterojunction is the most popular and efficient architecture due to the higher donor−acceptor interface area, where charge separation occurs.[17] Nowadays, the most common acceptor material used in bulk heterojunction solar cells is fullerene derivatives (like [6,6]-phenyl-C_{61}-butyric acid methyl ester, $PC_{61}BM$, and [6,6]-phenyl-C71-butyric acid methyl ester, $PC_{71}BM$),[18] commonly blended with an acceptor conjugated polymer like poly(3-hexylthiophene) (P3HT). Experimental results using transient absorption spectroscopy for the study of the charge-transfer process in these blends show that the charge carriers are generated within the time resolution of the instrument (∼100 fs).[19] Brabec et al. have also revealed an ultrafast charge-transfer process in a bulk heterojunction with a time constant of ∼45 fs using ultrafast spectroscopic techniques.[20] In both cases, the coherent nature of the oscillations is associated with phonon modes coupled to the electronic excitation of the conjugated polymer. Recent experimental and theoretical studies confirm that coherent vibronic coupling between electrons and nuclei is of key importance for the first steps of charge separation in covalent,[21] noncovalently[22] linked organic systems and also in inorganic materials like vertically stacked transition-metal dichalcogenide.[23,24] In the last several years, the PCE for this kind of organic solar cells surpassed 10% by developing novel p-type semiconductors (donors) but maintaining fullerenes as the acceptor material.[25,26]

In recent years, there was particular interest in developing new acceptor materials due to limited visible-light absorption, difficult functionalization, high production cost, and bad mechanical properties of the fullerene derivatives.[18] 3,4,9,10-

Received: April 4, 2018
Accepted: June 11, 2018
Published: June 11, 2018

© XXXX American Chemical Society

DOI: 10.1021/acs.jpclett.8b01043
J. Phys. Chem. Lett. 2018, 9, 3517−3524

Perylenetetracarboxylic acid diimides (PDIs) and their derivatives are promising acceptor materials due to their high visible-light absorption, good electron-accepting ability, high electron mobility, and strong thermal, chemical and photochemical stabilities.[27] Li et al. reviewed recent progress in nonfullerene acceptors for efficient OSC,[28] showing PCE of 8.3[29] and 9.15%[30] for blends composed of a widely used polymer donor and PDI derivatives as acceptors.

In this work, we present a computational study of a supramolecular arrangement composed of a hydrogenated nanodiamond interacting with a PDI molecule. The system shows ultrafast charge transfer on the scale of a few tens of femtoseconds after photoexcitation of the acceptor. This system therefore belongs to the same class of systems as the dyads and triads mentioned above. After the charge-transfer process, the system reaches a stable steady state showing extremely efficient charge separation, avoiding charge recombination processes in the studied time window. Because our method does not take into account nuclear motion, a pure electronic reordering of the of the system after charge separation is the reason for the irreversibility of the ultrafast charge-transfer process. A novel component of the system we show is that the hole acceptor is a nanosized diamond particle. Nanodiamonds are outstanding materials with properties like high surface area, surface structure tunability, excellent mechanical and optical properties, biocompatibility, and chemical stability.[31] The surface chemistry of nanodiamonds allows us to attach many different functional groups to their surface when compared with other carbon-based materials like nanotubes. For example, hydrogenated nanodiamonds can be obtained[32] as well as reactive C−F and C−Cl surfaces for wet chemistry functionalization.[33] This chemical versatility would allow us to further elaborate on the basic structure we show to ensure efficient and time-stable charge separation. Within light capture, nanodiamonds have attracted considerable interest as material for solar cells,[34] including applications as anodes,[35] p-type semiconductor[36] in OSC, and light-scattering material[37] in dye-sensitized solar cells (DSSCs).

The irreversibility of the light-induced charge-separation process is given by a three-stage mechanism. First, an electron hole pair is formed in the PDI molecule within the first 20 fs. This is then followed by electron transfer from a manifold of nanodiamond states (with energy tuned within the optical gap of the acceptor) within the next 20 fs. Then, pure electronic stabilization of the charge-separated state is caused by energy detuning between donor and acceptor states. Given the very large chemical hardness of diamond, its charging induces a large change in the relative energies between the donor states, whereas the acceptor state is only slightly modified in energy upon hole annihilation. This relative change in energy is the cause of rapid detuning of donor and acceptor states, stabilizing the charge-separated state. The mechanism works in a trap-door like fashion, in which an electron is transferred from the ND to the PDI but Rabi oscillations of the electron back to the nanodiamond are prevented by electrostatic detuning.

Diamond surface energies were calculated using a slab structure of at least 16 periodically repeated carbon layers and allowing 6 layers on each side of the slab to relax. This method was used by Kern and Hafner, who presented ab initio local-density-functional calculations of the electronic structure of clean and hydrogenated diamond (110) surfaces.[38] Here we performed the same calculations for three clean diamond low-index surfaces within the density functional tight-binding approach. Table 1 shows the diamond surfaces energies in comparison with the values obtained by Kern and Hafner. The results shows good agreement with ab initio results. Hence, our tight-binding approach can reproduce the structures and energies obtained with density functional theory (DFT).

Table 1. Surface Energies of Low-Index Diamond Surfaces (in eV per surface site) Calculated with DFTB Model[a]

diamond surface	present result	reference[b]
100 2db[c]	3.46	3.63
110 1db[c]	1.68	1.66
111 3db[c]	4.03	4.63

[a]Values obtained are compared with those presented in reference. [b]Kern and Hafner.[38] [c]db: dangling bonds.

It could be observed that the smallest surface energy corresponds to the 110 diamond face (1.68 eV per surface site). Taking this fact into account, we built nanodiamond structures of different sizes in a shape that maximizes the 110 surface-exposed. We observe previously that structures with multiple faces exposed show instability, probably due to a high edge energy between different faces for crystals of this size. The structures were hydrogen-passivated, obtaining stable nanodiamonds of irregular octahedral shape (similar to structures previously reported in literature[39,40]). These structures are shown in Figure 1a. To study the electronic properties, we calculated the density of states of the nanodiamonds (see Figure 1b). The DOS shows a typical "insulator" material with a large band gap. The quantum confinement effect is observed, which is in accordance with the trend observed by Fokin and Schreiner in ab initio band gap calculations of hydrogen-terminated nanodiamonds.[40] The larger the size, the smaller the band gap—from 10.9 eV for the smallest ND ($C_{26}H_{30}$) to 8.7 eV for the biggest ND ($C_{190}H_{110}$) studied here.

To study the optical properties, absorption spectra of the NDs were calculated and are displayed in Figure 1c. A decrease in the energy of the lowest energy excitation is observed as the nanodiamond size decreases. This agrees with the quantum confinement effect on the nanometer scale and the lowering of the band gap observed in Figure 1c (b).

Next, we build a donor + acceptor complex composed of a perylene tetracarboxylic diimide interacting with a hydrogen-terminated ND by London dispersion forces (see Figure 2a). Figure 2b displays the evolution of the Mulliken charge distributions in the ND (donor) and the PDI (acceptor) upon photoexcitation of the complex with time-dependent electric field pulse perturbation at 2.2 eV in resonance with the HOMO−LUMO transition of the PDI (as can be seen in the absorption spectra in Figure S2) and with an intensity of 0.1 V $Å^{-1}$. From Figure 2b, we observe that the acceptor molecule (PDI) becomes increasingly negatively charged as a function of time during the duration of the pulse; this charge transfer continues for a short time after the pulse, reaching a steady state after 90 fs. The opposite process occurs in the donor. A net charge is transferred from the ND to the PDI molecule. A similar process can be observed in an analogous covalently linked system (see Figure S1a,b). As can be seen from Figure S2, the lowest energy band that appears in the absorption spectrum is the PDI HOMO−LUMO transition; furthermore, no new bands appear upon the formation of the complex. This evidence suggest the absence of spurious charge-transfer

DOI: 10.1021/acs.jpclett.8b01043
J. Phys. Chem. Lett. 2018, 9, 3517−3524

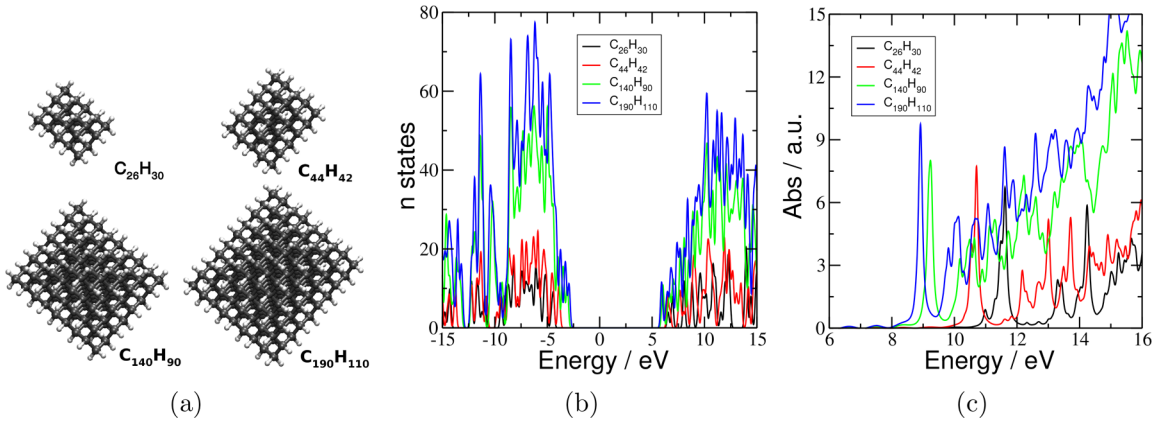

Figure 1. (a) Irregular octahedral nanodiamonds of different sizes.(b) Density of states for the ND structures. (c) Calculated spectra of the NDs.

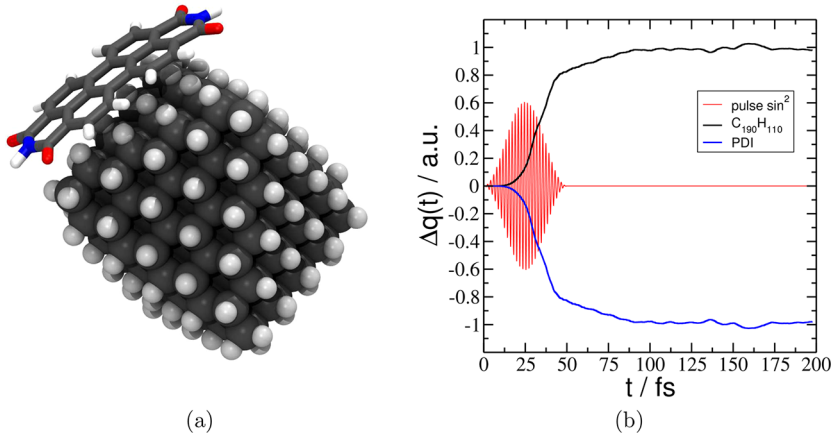

Figure 2. (a) Donor−acceptor complex, hydrogenated-ND + PDI. (b) Charge as a function of time for donor (black) and acceptor (blue). The squared-sinusoidal pulse perturbation in tune with the HOMO−LUMO transition of the acceptor is represented in red.

excitations in this particular system and that the calculated excited-state structure is correct. We must stress that the described charge-transfer process occurs once a significant population has been transferred from the HOMO to the LUMO of the PDI. It does not correspond to a charge-transfer excitation but to a dynamic process of energy reorganization that happens after the excitation and therefore outside the scope of a linear response description. Monitoring the dipole moments of the donor and the acceptor, we see that the steady state is a dynamic state because the dipole moment of the acceptor keeps oscillating after charge-transfer process is complete (see Figure S3).

Three things are remarkable in this process. The first one is the amount of charge transferred, one full electron. The second is the time scale of the process; <90 fs is needed to complete the transference, and 80% of the charge is transferred within <50 fs. Third, the system reaches a stable steady state after the pulse perturbation ends, which lasts for the whole simulation time. In other words, the charge separation seems to be extremely efficient in the system proposed, avoiding any charge recombination process on these time scales. The evidence discards a charge-transfer excitation because at the excitation energy at which the pulse is tuned the only active excitation is the HOMO−LUMO excitation of the acceptor (and the time scale of a charge-transfer excitation would be on the order of a few femtoseconds). The time scale of the process and the fact that nuclear motion is not taken into account point to a new photoinduced charge transfer mechanism. All of these data leads us to believe that there must be a pure electronic reordering of the electronic structure of the system that enhances charge separation, preventing charge recombination and leading to a stable steady-state in a trap-door like mechanism.

We also have studied the process dependence with the field intensity and pulse duration. As the field intensity increases, the positive charge reached for the donor at the steady-state increases (see Figure S4). As the pulse width increases, the positive charge reached for the donor at the steady-state increases as well, but it takes more time to achieve the charge separated state (see Figure S5). The amount of transferred charge exponentially depends on the distance between donor and acceptor, as can be expected from the decrease in electronic coupling between the two; see Figure S6. We additionally investigate the dependence of the process on the nanodiamond size, observing a decrease in the steady-state charge as the nanodiamond size decreases (see Figure S7). This decrease in steady-state charge with size is related to the lower density of ND donor states within the optical gap for smaller structures. To discard the possibility that a particular arrangement causes this unusual process, we studied the configuration space of the smallest complex ($C_{26}H_{30}$+PDI). We performed Born−Oppenheimer molecular dynamics at 500 K, took random configurations from this trajectory, and performed the corresponding electron dynamics. (For further

DOI: 10.1021/acs.jpclett.8b01043
J. Phys. Chem. Lett. 2018, 9, 3517−3524

details of the molecular dynamics, see Section S2.6 in the Supporting Information.) We find that the charge-transfer process is not a characteristic of a particular configuration but that it is geometry-independent to the extent explored by the performed sampling (see Figure S8).

To further investigate the charge-transfer mechanism, we studied the evolution of the density matrix in the molecular orbital basis set. This study provides a more detailed understanding of the nature of the excitation. We have used this method in previous works for a complete characterization of the type of injection mechanism in DSSC[41] and for a deeper understanding of the molecular orbitals involved in the excitation of photosynthetic pigments outside the scope of the Fermi golden rule.[42]

Figure 3 (lower graph) shows the time-dependent molecular orbital populations for the donor + acceptor complex (Figure 2a, left) when a pulse perturbation in tune with the excitation energy of the acceptor is applied. The upper graph in Figure 3 shows the evolution of the donor charge (ND). From Figure 3, we can divide the process into three stages. The first stage is a preparation step (from 0 to 20 fs); the charge of the donor remains close to zero during this stage, but population transfer can be observed from the HOMO to the LUMO of the acceptor (black and red curves). After that, we can see a whole reorganization of several states in the charge-transfer stage (from 20 to 50 fs). Many states are involved in this process. Finally, we found the stabilization stage, where the charge of the donor reached a steady state (see Figure 2b) over 100 fs with an accompanying change in a broad manifold of the molecular orbitals. After the steady state is reached, molecular orbital populations remain steady around an average value, with fast oscillations that correspond to the carrier frequency of the pulse (not shown in the Figure).

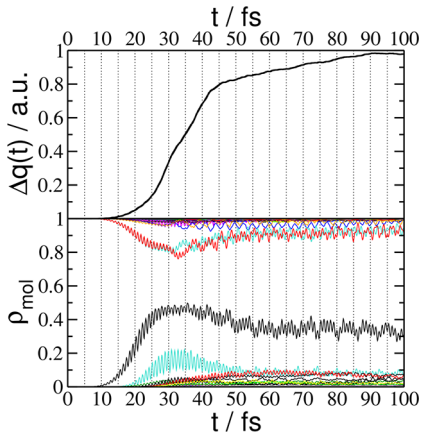

Figure 3. (Upper graph) Donor charge as a function of time. (Lower graph) GS orbital population as a function of time for the donor−acceptor complex. The basis used is constructed from the molecular orbitals of the ground state.

To gain insight into the electronic nature of the process, we calculated the projected density of states (PDOS) of the ground state and the corresponding cationic and anionic states of the system. Figure 4a,b shows the evolution of the PDOS as the negative and positive charge of the system increases, respectively. At the neutral state, the nanodiamond has plenty of states to donate charge, located at the optical gap of the acceptor, enhancing the charge-transfer process. As the system charges, an electronic reordering takes place, which leads to an energy change of the states. The nanodiamond states change their energies, leaving the optical gap. The number of states that leaves the gap for the largest system studied is 45 for the case of a negatively charged system and 13 for the case of a positively charged system. This reduction in the states within the optical gap avoids the inverse transfer process, rapidly and irreversibly reaching the steady state we have seen in Figure 2b. In other words, these states can transfer charge to the acceptor until they detune from the optical gap.

The random surface substitution of H atoms by F strongly affects the charge dynamic of the system. We built ND + PDI complexes with different F percentages in the nanodiamond surface (see Section S3.1 in the Supporting Information). Then, we calculated the charge transfer upon photostimulation and compared the dynamics obtained with the purely hydrogenated-ND + PDI complex.

Figure 5 shows the evolution of the Mulliken charge distribution in the ND (donor) upon the photoexcitation of the fluorinated complexes with a pulse time-dependent electric

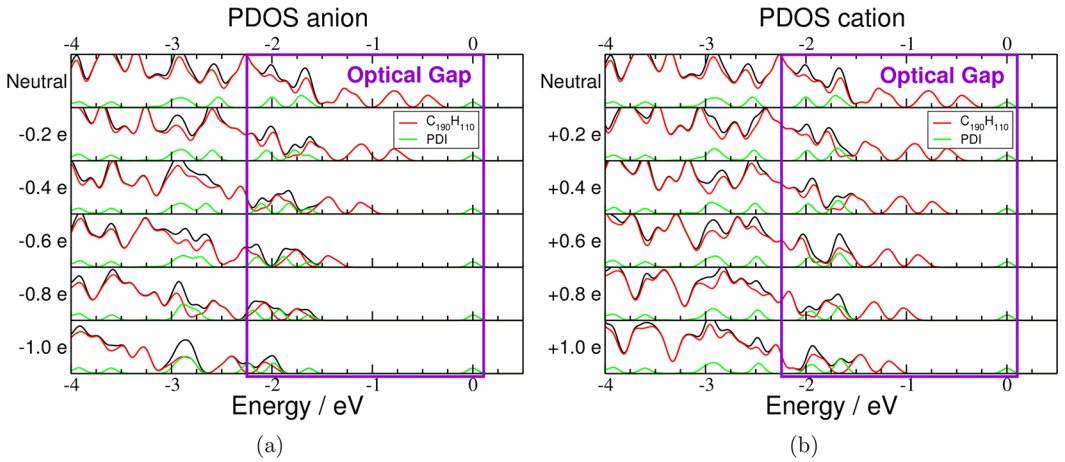

Figure 4. Projected density of states (PDOS) for the hydrogenated-ND + PDI complex for different partial amounts of charge. (a) Negative partial charge values. (b) Positive partial charge values. Nanodiamond PDOS in red, PDI PDOS in green, total DOS in black. Charges are decremented or incremented in 0.2 e steps. The rectangles in each Figure highlight the optical gap of the acceptor molecule (PDI). In all cases, the PDOS are referenced to the LUMO energy of the system.

DOI: 10.1021/acs.jpclett.8b01043
J. Phys. Chem. Lett. 2018, 9, 3517−3524

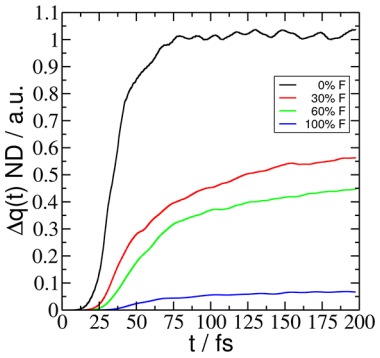

Figure 5. Donor charge as a function of time for different fluorination percentages of the nanodiamonds.

field perturbation in tune with the acceptor excitation energy. The charge transferred decreases strongly as the F percentage on the surface increases, reaching an order of magnitude difference between the fully hydrogenated-ND and the fully fluorinated-ND. Besides the decrease in the amount of charge transferred, fluorinated-NDs do not reach a steady-state within the 200 fs simulation window as the hydrogenated-NDs do.

These results show the effect of the surface fluorination in the electronic properties of the ND. The strong electronegativity of the F moves the ND surface states energies to more negative values, as shown in Figure S10 for the PDOS evolution of the anion and cation total fluorinated-ND + PDI complex. It can be observed that for the neutral complex there are no nanodiamond states in the optical gap of the acceptor. This fact avoids the charge-transfer mechanism described above, showing a completely different charge dynamic through time, as can be seen in Figure 5. As a consequence, the system does not reach a steady state within the simulated time window and significantly decreases the total transferred charge.

The evidence allows us to propose a three-stage trap-door-like irreversible charge transfer in which an electron hole pair is first created at the PDI, then the hole is filled by available electrons from a manifold of ND states that are close in energy, which then detune. This detuning process upon charge separation is the key for the trap door mechanism. The working principle requires that donor and acceptor have adequate ionization energies and electron affinities to ensure the directionality of charge transfer. Furthermore, the chemical hardness of the donor (2.41 eV) and acceptor (5.51 eV) systems differs substantially. The hardness is calculated as[43] $\eta = \frac{1}{2}\left(\frac{\partial \mu}{\partial N}\right) = \frac{I-A}{2}$, where I and A are the ionization energy and electronic affinity, respectively. This difference in hardness ensures that charging of the donor produces a large change in relative energies between donor and acceptor, causing a sudden detuning of these states, which is the cause for the observed irreversibility of the process.

Our simulations do not take into account the possibility of nuclear motion. Given the fact that most of the charge transfer happens over a very short period of time, we would expect, based on our experience of how systems react to such sudden changes in electronic structure, coherent breathing oscillations to be launched impulsively in both systems.[44] The effect of these would increase the detuning (given by the sudden nuclear motion) on one side (helping the transfer) but lower the hardness of the ND on the other side (because a new degree of freedom over which the system can relax would be added). It is very hard to assess the relative importance of these two processes. An estimation of the importance of the second effect can be assessed perturbatively by recalculating the values of hardness by relaxing the geometries of the respective anion and cation. The new values of hardness are 3.12 and 4.61 eV for the PDI and ND, respectively. This would indicate that incorporating nuclear motion might reduce the amount of transferred charge via a reduction of the effective hardness difference between donor and acceptor.

Within the present work, we have studied the charge-transfer process between irregular octahedral nanodiamond structures (as donor) and an organic common dye like PDI (as acceptor), performing simulations of the time-evolving electronic structure under visible irradiation. The main result shows an ultrafast charge transfer in the hydrogenated-ND + PDI complex. The system reaches a stable steady-state in <90 fs, transferring one electron from the donor to the acceptor after the pulse irradiation. The charge separation is extremely fast and efficient in this system, related to a resonance and the subsequent separation of states. These results show that is possible to obtain an stable charge-separated state enhanced only by a pure electronic reorganization of the system, without polaron formation or nuclear relaxation, by a purely electronic trap-door like mechanism in which donor and acceptor orbitals dynamically respond to the transferred charge, suddenly detuning precluding charge recombination. To the best of our knowledge, this is the very first time that this phenomenon has been described.

Our information at present, limited by the time windows of the simulation, does not allow us to reach into longer times and assess the importance of processes such as back-electron transfer that may occur on the picosecond to nanosecond time scales. We believe that the present system (as is the case of the triads that are described in the first paragraphs of the paper) is just a possible component of a bigger light-harvesting structure that stabilizes and further separates the charge via, for example, a chain of redox reactions or other mechanisms, such as those that take place in photosynthetic reaction centers and dye-sensitized or organic solar cells.

A trap-door like mechanism is proposed by which the charge-transfer state is stabilized electrostatically in a dynamic fashion by the charge-separation-induced detuning of donor and acceptor states. The mechanism requires the combination of a donor−acceptor pair with very different chemical hardness. In the case shown here, the PDI system is chemically soft and can accommodate charge easily, but the nanodiamond system states respond strongly to charging. This difference in response between the two systems provides the driving force for the purely electronic stabilization of the charge-transfer state. Another requisite is that the donor has a manifold of states initially in tune with the acceptor optical gap that can transfer charge; this manifold acts as a reservoir that can fill the hole while detuning. (A single donor state would immediately detune.) The hard system is then also required to be a nanosystem with a large density of states in tune with the acceptor.

This phenomenon could be extremely useful in electronic applications where the efficient irreversible charge separation is critical, like light-harvesting devices. We demonstrate that the process strongly depends on the ND surface structure, showing that fluorinated NDs never reach a steady state within the simulated time window and transfer an order of magnitude less charge than the hydrogenated ND under the same conditions,

DOI: 10.1021/acs.jpclett.8b01043
J. Phys. Chem. Lett. 2018, 9, 3517−3524

pointing to the fact that the charge-transfer efficiency can be tuned using surface modifications with differing electronegativity. Further comprehension of this kind of stabilization is now needed. There are opened questions like: Are there other systems where we can observed this phenomenon? Can we observe the same experimentally? We believe that the presence of nanodiamonds in a PDI solution should cause strong quenching of the PDI fluorescence. This could be a first step toward an experimental verification of the studied phenomenon.

COMPUTATIONAL METHODS

The self-consistent-charge density-functional-tight-binding (SCC-DFTB) method was used to describe the electronic structure of the ground state (GS) in all studied systems.[45−47] On the basis of a controlled approximation of DFT, this method has been used with success to describe quantum properties and electronic structures of large organic and bioinorganic systems.[47,48] We compute the GS Hamiltonian (H_{GS}) and overlap matrix (S) using the DFTB+ package,[49] which is an implementation of the SCC-DFTB method. With the H_{GS} and the S matrix, we can obtain the initial GS reduced single-electron density matrix (ρ). The pbc-0-3 DFTB parameter set was employed to obtain the electronic structure of the nanodiamonds and organic molecules presented in this work.

Starting from the initial ρ, we can obtain the excited-state properties of a system, applying an external perturbation and monitoring the evolution of the density matrix through time. In other words, a real-time propagation of the reduced single-electron density matrix (ρ) under the influence of a time-varying external field allows us to describe electronic dynamics of the whole system. This method has been used and described in the past by us[41,42,50−59] and others by propagating molecular orbitals instead of the single-electron density matrix[60] and in a linear response framework.[61] The light−matter interaction in the DFTB approach that we use is incorporated in the Hamiltonian in the dipole approximation as

$$\hat{H}(t) = \hat{H}^{\mathrm{DFTB}}(\hat{\rho}(t)) - \hat{\boldsymbol{\mu}}\cdot\mathbf{E}(t)$$

where $\hat{\boldsymbol{\mu}}$ is the operator that, when traced with the density matrix, generates the dipole moment of the Mulliken charges

$$\mathrm{Tr}[\hat{\boldsymbol{\mu}}\hat{\rho}] = \sum_I \mathbf{r}_I \delta q_i$$

In this way, the time-dependent external electric field enters the dynamics explicitly on the atomic orbital basis.

In particular, the absorption spectra of the systems presented in this work were obtained after the application of an initial perturbation in the shape of a delta Dirac. The intensity of this perturbation was 0.001 V Å^{-1} (within the linear response regime). The nonequilibrium properties, as the charge-transfer processes, were calculated after the application of an initial perturbation in the shape of a squared-sinusoidal pulse of 50 fs in all cases. The intensity of this perturbation was 0.1 V Å^{-1}, equivalent to 1.35×10^{11} W/cm^2 (out of the linear response regime).

ASSOCIATED CONTENT

Supporting Information

The Supporting Information is available free of charge on the ACS Publications website at DOI: 10.1021/acs.jpclett.8b01043.

Additional data and characterization for the systems studied (PDF)

AUTHOR INFORMATION

Corresponding Author

*E-mail: cgsanchez@fcq.unc.edu.ar.

ORCID

Carlos R. Medrano: 0000-0001-7696-8366

Cristián G. Sánchez: 0000-0001-7616-1802

Notes

The authors declare no competing financial interest.

ACKNOWLEDGMENTS

We acknowledge financial support from SeCyT UNC. This work used computational resources from CCAD - Universidad Nacional de Córdoba (http://ccad.unc.edu.ar/), in particular, the Mendieta Cluster, which is part of SNCAD - MinCyT, República Argentina. C.R.M. is grateful for a studentship from CONICET.

REFERENCES

(1) Blankenship, R. E. *Molecular Mechanisms of Photosynthesis*; Wiley/Blackwell: Chichester, U.K., 2008; pp 1−321.

(2) Tabushi, I.; Koga, N.; Yanagita, M. Efficient Intramolecular Quenching and Electron Transfer in Tetraphenylporphyrin Attached with Benzoquinone or Hydroquinone as a Photosystem Model. *Tetrahedron Lett.* **1979**, *20*, 257−260.

(3) Kong, J. L. Y.; Loach, P. A. Syntheses of covalently-linked porphyrin-quinone complexes. *J. Heterocycl. Chem.* **1980**, *17*, 737−744.

(4) Liddell, P. a.; Sumida, J. P.; Macpherson, A. N.; Noss, L.; Seely, G. R.; Clark, K. N.; Moore, A. L.; Moore, T. a.; Gust, D. Preparation and Photophysical Studies of Porphyrin-C 60 Dyads. *Photochem. Photobiol.* **1994**, *60*, 537−541.

(5) Hermant, R. M.; Liddell, P. A.; Lin, S.; Alden, R. G.; Kang, H. K.; Moore, A. L.; Moore, T. A.; Gust, D. Mimicking Carotenoid Quenching of Chlorophyll Fluorescence. *J. Am. Chem. Soc.* **1993**, *115*, 2080−2081.

(6) Cowan, J. A.; Sanders, J. K. M. Pyromellitimide-bridged porphyrins as model photosynthetic systems. 1. Synthesis and steady state fluorescence properties. *J. Chem. Soc., Perkin Trans. 1* **1985**, 2435−2437.

(7) Moore, T. A.; Gust, D.; Mathis, P.; Mialocq, J. C.; Chachaty, C.; Bensasson, R. V.; Land, E. J.; Doizi, D.; Liddell, P. A.; Lehman, W. R.; et al. Photodriven charge separation in a carotenoporphyrin-quinone triad. *Nature* **1984**, *307*, 630−632.

(8) Carbonera, D.; Di Valentin, M.; Corvaja, C.; Agostini, G.; Giacometti, G.; Liddell, P. A.; Kuciauskas, D.; Moore, A. L.; Moore, T. A.; Gust, D. EPR investigation of photoinduced radical pair formation and decay to a triple state in a carotene-porphyrin-fullerene triad. *J. Am. Chem. Soc.* **1998**, *120*, 4398−4405.

(9) Gust, D.; Moore, T. A.; Moore, A. L. Mimicking photosynthetic solar energy transduction. *Acc. Chem. Res.* **2001**, *34*, 40−48.

(10) Kodis, G.; Liddell, P. a.; Moore, A. L.; Moore, T. a.; Gust, D. Synthesis and photochemistry of a carotene−porphyrin−fullerene model photosynthetic reaction center. *J. Phys. Org. Chem.* **2004**, *17*, 724−734.

(11) Kuciauskas, D.; Liddell, P. A.; Lin, S.; Johnson, T. E.; Weghorn, S. J.; Lindsey, J. S.; Moore, A. L.; Moore, T. A.; Gust, D. An artificial

DOI: 10.1021/acs.jpclett.8b01043
J. Phys. Chem. Lett. 2018, 9, 3517−3524

photosynthetic antenna-reaction center complex. *J. Am. Chem. Soc.* **1999**, *121*, 8604−8614.
(12) D'Souza, F.; Chitta, R.; Ohkubo, K.; Tasior, M.; Subbaiyan, N. K.; Zandler, M. E.; Rogacki, M. K.; Gryko, D. T.; Fukuzumi, S. Corrole- Fullerene Dyads: Formation of Long- Lived charge-Separated States in Nonpolar Solvents. *J. Am. Chem. Soc.* **2008**, *130*, 14263.
(13) Kuciauskas, D.; Liddell, P.; Lin, S.; Stone, S.; Moore, A.; Moore, T.; Gust, D. Photoinduced Electron Transfer in Carotenoporphyrin-Fullerene Triads: Temperature and Solvent Effects. *J. Phys. Chem. B* **2000**, *104*, 4307−4321.
(14) Roncali, J. Single material solar cells: The next frontier for organic photovoltaics? *Adv. Energy Mater.* **2011**, *1*, 147−160.
(15) Narayanaswamy, K.; Venkateswararao, A.; Nagarjuna, P.; Bishnoi, S.; Gupta, V.; Chand, S.; Singh, S. P. An Organic Dyad Composed of Diathiafulvalene-Functionalized Diketopyrrolopyrrole−Fullerene for Single-Component High-Efficiency Organic Solar Cells. *Angew. Chem., Int. Ed.* **2016**, *55*, 12334−12337.
(16) Lin, Y.; Li, Y.; Zhan, X. Small molecule semiconductors for high-efficiency organic photovoltaics. *Chem. Soc. Rev.* **2012**, *41*, 4245.
(17) Hoppe, H.; Sariciftci, N. S. Organic solar cells: An overview. *J. Mater. Res.* **2004**, *19*, 1924−1945.
(18) Chen, W.; Zhang, Q. Recent progress in non-fullerene small molecule acceptors in organic solar cells (OSCs). *J. Mater. Chem. C* **2017**, *5*, 1275−1302.
(19) Kaake, L. G.; Moses, D.; Heeger, A. J. Coherence and uncertainty in nanostructured organic photovoltaics. *J. Phys. Chem. Lett.* **2013**, *4*, 2264−2268.
(20) Brabec, C. J.; Zerza, G.; Cerullo, G.; De Silvestri, S.; Luzzati, S.; Hummelen, J. C.; Sariciftci, S. Tracing photoinduced electron transfer process in conjugated polymer/fullerene bulk heterojunctions in real time. *Chem. Phys. Lett.* **2001**, *340*, 232−236.
(21) Rozzi, C. A.; Falke, S. M.; Spallanzani, N.; Rubio, A.; Molinari, E.; Brida, D.; Maiuri, M.; Cerullo, G.; Schramm, H.; Christoffers, J.; et al. Quantum coherence controls the charge separation in a prototypical artificial light-harvesting system. *Nat. Commun.* **2013**, *4*, 1602.
(22) Falke, S. M.; Rozzi, C. A.; Brida, D.; Maiuri, M.; Amato, M.; Sommer, E.; De Sio, A.; Rubio, A.; Cerullo, G.; Molinari, E.; et al. Coherent ultrafast charge transfer in an organic photovoltaic blend. *Science* **2014**, *344*, 1001−1005.
(23) Long, R.; Prezhdo, O. V. Quantum Coherence Facilitates Efficient Charge Separation at a MoS_2/$MoSe_2$ van der Waals Junction. *Nano Lett.* **2016**, *16*, 1996−2003.
(24) Zheng, Q.; Saidi, W. A.; Xie, Y.; Lan, Z.; Prezhdo, O. V.; Petek, H.; Zhao, J. Phonon-Assisted Ultrafast Charge Transfer at van der Waals Heterostructure Interface. *Nano Lett.* **2017**, *17*, 6435−6442.
(25) He, Z.; Xiao, B.; Liu, F.; Wu, H.; Yang, Y.; Xiao, S.; Wang, C.; Russell, T. P.; Cao, Y. Single-junction polymer solar cells with high efficiency and photovoltage. *Nat. Photonics* **2015**, *9*, 174−179.
(26) Liao, S. H.; Jhuo, H. J.; Yeh, P. N.; Cheng, Y. S.; Li, Y. L.; Lee, Y. H.; Sharma, S.; Chen, S. A. Single junction inverted polymer solar cell reaching power conversion efficiency 10.31% by employing dual-doped zinc oxide nano-film as cathode interlayer. *Sci. Rep.* **2015**, *4*, 4−10.
(27) Zhang, X.; Lu, Z.; Ye, L.; Zhan, C.; Hou, J.; Zhang, S.; Jiang, B.; Zhao, Y.; Huang, J.; Zhang, S.; et al. A potential perylene diimide dimer-based acceptor material for highly efficient solution-processed non-fullerene organic solar cells with 4.03% efficiency. *Adv. Mater.* **2013**, *25*, 5791−5797.
(28) Li, S.; Liu, W.; Li, C.-Z.; Shi, M.; Chen, H. Efficient Organic Solar Cells with Non-Fullerene Acceptors. *Small* **2017**, *13*, 1701120.
(29) Meng, D.; Fu, H.; Xiao, C.; Meng, X.; Winands, T.; Ma, W.; Wei, W.; Fan, B.; Huo, L.; Doltsinis, N. L.; et al. Three-Bladed Rylene Propellers with Three-Dimensional Network Assembly for Organic Electronics. *J. Am. Chem. Soc.* **2016**, *138*, 10184−10190.
(30) Duan, Y.; Xu, X.; Yan, H.; Wu, W.; Li, Z.; Peng, Q. Pronounced Effects of a Triazine Core on Photovoltaic Performance−Efficient Organic Solar Cells Enabled by a PDI Trimer-Based Small Molecular Acceptor. *Adv. Mater.* **2017**, *29*, 1605115.
(31) Mochalin, V. N.; Shenderova, O.; Ho, D.; Gogotsi, Y. The properties and applications of nanodiamonds. *Nat. Nanotechnol.* **2012**, *7*, 11−23.
(32) Arnault, J.-C.; Petit, T.; Girard, H.; Chavanne, A.; Gesset, C.; Sennour, M.; Chaigneau, M. Surface chemical modifications and surface reactivity of nanodiamonds hydrogenated by CVD plasma. *Phys. Chem. Chem. Phys.* **2011**, *13*, 11481−11487.
(33) Liu, Y.; Gu, Z.; Margrave, J. L.; Khabashesku, V. N. *Chem. Mater.* **2004**, *16*, 3924−3930.
(34) Kausar, A. Nanodiamond: a multitalented material for cutting edge solar cell application. *Mater. Res. Innovations* **2017**, *8917*, 1−13.
(35) Lim, C. H. Y. X.; Zhong, Y. L.; Janssens, S.; Nesladek, M.; Loh, K. P. Oxygen-terminated nanocrystalline diamond film as an efficient anode in photovoltaics. *Adv. Funct. Mater.* **2010**, *20*, 1313−1318.
(36) Nagata, A.; Oku, T.; Kikuchi, K.; Suzuki, A.; Yamasaki, Y.; Osawa, E. Fabrication, nanostructures and electronic properties of nanodiamond-based solar cells. *Prog. Nat. Sci.* **2010**, *20*, 38−43.
(37) Karimi Tafti, M. H.; Sadeghzadeh, S. M. Novel use of nanodiamonds as light-scattering material in dye-sensitized solar cells. *J. Mater. Sci.: Mater. Electron.* **2016**, *27*, 5225−5232.
(38) Kern, G.; Hafner, J. Ab initio calculations of the atomic and electronic structure of clean and hydrogenated diamond (110) surfaces. *Phys. Rev. B: Condens. Matter Mater. Phys.* **1997**, *56*, 4203−4210.
(39) Areshkin, D. A.; Shenderova, O. A.; Adiga, S. P.; Brenner, D. W. Electronic properties of diamond clusters: Self-consistent tight binding simulation. *Diamond Relat. Mater.* **2004**, *13*, 1826−1833.
(40) Fokin, A. A.; Schreiner, P. R. Band gap tuning in nanodiamonds: first principle computational studies. *Mol. Phys.* **2009**, *107*, 823−830.
(41) Oviedo, M. B.; Zarate, X.; Negre, C. F. A.; Schott, E.; Arratia-Pérez, R.; Sánchez, C. G. Quantum Dynamical Simulations as a Tool for Predicting Photoinjection Mechanisms in Dye-Sensitized TiO 2 Solar Cells. *J. Phys. Chem. Lett.* **2012**, *3*, 2548−2555.
(42) Oviedo, M. B.; Sánchez, C. G. Transition dipole moments of the Qy band in photosynthetic pigments. *J. Phys. Chem. A* **2011**, *115*, 12280−12285.
(43) Parr, R. G.; Yang, W. *Density Functional Theory of Atoms and Molecules*; Oxford University Press, 1989.
(44) Bonafe, F. P.; Aradi, B.; Guan, M.; Douglas-Gallardo, O. A.; Lian, C.; Meng, S.; Frauenheim, T.; Sanchez, C. G. Plasmon-driven sub-picosecond breathing of metal nanoparticles. *Nanoscale* **2017**, *9*, 12391−12397.
(45) Elstner, M.; Porezag, D.; Jungnickel, G.; Elsner, J.; Haugk, M.; Frauenheim, T.; Suhai, S.; Seifert, G. Self-consistent-charge density-functional tight-binding method for simulations of complex materials properties. *Phys. Rev. B: Condens. Matter Mater. Phys.* **1998**, *58*, 7260−7268.
(46) Elstner, M.; Seifert, G. Density functional tight binding. *Philos. Trans. R. Soc., A* **2014**, *372*, 20120483.
(47) Christensen, A. S.; Kubař, T.; Cui, Q.; Elstner, M. Semiempirical Quantum Mechanical Methods for Noncovalent Interactions for Chemical and Biochemical Applications. *Chem. Rev.* **2016**, *116*, 5301−5337.
(48) Gaus, M.; Cui, Q.; Elstner, M. Density functional tight binding: Application to organic and biological molecules. *Wiley Interdisciplinary Reviews: Computational Molecular Science* **2014**, *4*, 49−61.
(49) Aradi, B.; Hourahine, B.; Frauenheim, T. DFTB+, a sparse matrix-based implementation of the DFTB method. *J. Phys. Chem. A* **2007**, *111*, 5678−5684.
(50) Oviedo, M. B.; Negre, C. F. a.; Sánchez, C. G. Dynamical simulation of the optical response of photosynthetic pigments. *Phys. Chem. Chem. Phys.* **2010**, *12*, 6706−11.
(51) Negre, C. F. a.; Fuertes, V. C.; Oviedo, M. B.; Oliva, F. Y.; Sánchez, C. G. Quantum Dynamics of Light-Induced Charge Injection in a Model Dye−Nanoparticle Complex. *J. Phys. Chem. C* **2012**, *116*, 14748−14753.

DOI: 10.1021/acs.jpclett.8b01043
J. Phys. Chem. Lett. 2018, 9, 3517−3524

(52) Fuertes, V. C.; Negre, C. F. a.; Oviedo, M. B.; Bonafé, F. P.; Oliva, F. Y.; Sánchez, C. G. A theoretical study of the optical properties of nanostructured TiO2. *J. Phys.: Condens. Matter* **2013**, *25*, 115304.
(53) Negre, C. F. A.; Perassi, E. M.; Coronado, E. A.; Sánchez, C. G. Quantum dynamical simulations of local field enhancement in metal nanoparticles. *J. Phys.: Condens. Matter* **2013**, *25*, 125304.
(54) Primo, E. N.; Oviedo, M. B.; Sánchez, C. G.; Rubianes, M. D.; Rivas, G. A. Bioelectrochemical sensing of promethazine with bamboo-type multiwalled carbon nanotubes dispersed in calf-thymus double stranded DNA. *Bioelectrochemistry* **2014**, *99*, 8−16.
(55) Negre, C. F. A.; Young, K. J.; Oviedo, M. B.; Allen, L. J.; Sánchez, C. G.; Jarzembska, K. N.; Benedict, J. B.; Crabtree, R. H.; Coppens, P.; Brudvig, G. W.; et al. Photoelectrochemical hole injection revealed in polyoxotitanate nanocrystals functionalized with organic adsorbates. *J. Am. Chem. Soc.* **2014**, *136*, 16420−16429.
(56) Medrano, C. R.; Oviedo, M. B.; Sánchez, C. G. Photoinduced charge-transfer dynamics simulations in noncovalently bonded molecular aggregates. *Phys. Chem. Chem. Phys.* **2016**, *18*, 14840−14849.
(57) Mansilla Wettstein, C.; Bonafé, F. P.; Oviedo, M. B.; Sánchez, C. G. Optical properties of graphene nanoflakes: Shape matters. *J. Chem. Phys.* **2016**, *144*, 224305.
(58) Douglas-Gallardo, O. A.; Berdakin, M.; Sánchez, C. G. Atomistic Insights into Chemical Interface Damping of Surface Plasmon Excitations in Silver Nanoclusters. *J. Phys. Chem. C* **2016**, *120*, 24389−24399.
(59) Berdakin, M.; Taccone, M. I.; Pino, G. A.; Sánchez, C. G. DNA-protected silver emitters: charge dependent switching of fluorescence. *Phys. Chem. Chem. Phys.* **2017**, *19*, 5721−5726.
(60) Niehaus, T. A.; Heringer, D.; Torralva, B.; Frauenheim, T. Importance of electronic self-consistency in the TDDFT based treatment of nonadiabatic molecular dynamics. *Eur. Phys. J. D* **2005**, *35*, 467−477.
(61) Niehaus, T. A.; Suhai, S.; Della Sala, F.; Lugli, P.; Elstner, M.; Seifert, G.; Frauenheim, T. Tight-binding approach to time-dependent density-functional response theory. *Phys. Rev. B: Condens. Matter Mater. Phys.* **2001**, *63*, 085108.

DOI: 10.1021/acs.jpclett.8b01043
J. Phys. Chem. Lett. 2018, 9, 3517−3524